Electrostatic interactions and stability of dusty plasmas and the multicomponent Ornstein–Zernike equation

Anatoly V. Filippov [ID], Vladimir E. Fortov, Victor V. Reshetniak [ID], Andrey N. Starostin, and Igor M. Tkachenko [ID]

View Online   Export Citation   CrossMark

ARTICLES YOU MAY BE INTERESTED IN

Electrostatic interactions and stability of dusty plasmas and the multicomponent Ornstein–Zernike equation

View Online   Export Citation   CrossMark

Anatoly V. Filippov,[1,2,a)] (ID) Vladimir E. Fortov,[1] Victor V. Reshetniak,[2] (ID) Andrey N. Starostin,[1,2,b)]
and Igor M. Tkachenko[3] (ID)

AFFILIATIONS

[1] Joint Institute for High Temperatures, Russian Academy of Sciences, 125412 Moscow, Russia

[2] Troitsk Institute for Innovation and Fusion Research, Troitsk, 108840 Moscow, Russia

[3] Departament de Matemàtica Aplicada, Universitat Politècnica de València, 46022 Valencia, Spain

[a)] Author to whom correspondence should be addressed: fav@triniti.ru
[b)] Deceased.

ABSTRACT

Using the Ornstein–Zernike integral fluid equation for multi-component plasma, the dielectric properties and thermodynamical stability of dusty plasmas are studied. For the most non-ideal dust plasma subsystem, a transition to the one-component approximation is carried out. It is shown that the effective pseudopotential for determining the correlation functions in the selected subsystem should not include the contribution of this subsystem to the screening constant but also take into account the condition of total plasma quasineutrality. It is demonstrated that when the coupling parameter of the dust subsystem is smaller than unity, $\Gamma_{00} < 1$, the interaction potential between the charged plasma particles is fairly well described by the Debye potential with a full screening constant. For $\Gamma_{00} > 1$, the static dielectric function in the long wavelength domain becomes negative, and this domain expands when Γ_{00} increases. This leads to the appearance of attraction of particles with charges of the same sign and repulsion of particles with charges of the opposite sign. In this case, both the total pressure and the isothermal compressibility in the entire studied range of the coupling parameter $\Gamma_{00} < 250$ remain positive, but the isothermal compressibility of the dust subsystem becomes negative at $\Gamma_{00} \approx 2$ within the studied range of variation of the plasma parameters. The sign of the derivative of the chemical potential with respect to the total number of dust particles, the positiveness of which is the third condition for the thermodynamic stability, is shown to coincide with the sign of the isothermal compressibility of the dust subsystem. Therefore, it is concluded that the equilibrium dusty plasma at $\Gamma_{00} > 2$ is thermodynamically unstable.

I. INTRODUCTION

Plasmas, which contain the so-called condensed disperse phase or dusty plasmas, are widely spread in nature and used in technology, and therefore, research of such complex systems is of considerable interest both for fundamental physics[1–5] and for a number of applications, for example, in the nanoparticle industry.[6] The theoretical study of the charged particle interactions in such systems is still one of the most important issues.[7–13] Numerical studies of dusty plasmas by, for example, the molecular and Brownian dynamics methods are traditionally carried out with the interaction between charged heavy (dust) particles modeled by the pair Yukawa or Debye interaction potential (see, e.g., Refs. [14–20]) or with some additional interaction potential with the inverse squared interparticle distance asymptotic form at large distances (see, e.g., Ref. [21]). This model potential is applicable if the Debye–Hückel approximation[22] is applicable, and its validity at higher values of the coupling parameter of the dust subsystem raises questions.

The present work, unlike the above papers, is dedicated to the description of electrostatic properties of dusty plasmas with the Coulomb pair interaction potential between charged plasma particles based on the multicomponent Ornstein–Zernike equation.[23,24]

It was shown in Refs. [25] and [26] that the Ornstein–Zernike (OZ) equation in the hypernetted chain (HNC) approximation describes the thermodynamic properties of dusty plasmas quite well even up to the coupling parameter values of the order of 100. Therefore, it is exactly the HNC approximation, which is employed to close the system of OZ equations in this paper.

The Ornstein–Zernike equation is often employed to study multicomponent plasmas (mainly two-, rarely three-component plasmas, see, for example, Refs. [27–35] and references therein). In the present paper, the transition to a one-component description of the strongly coupled subsystem and the thermodynamic stability (TDS) of the multicomponent dusty plasma are described in detail and, as far as we know, for the first time. Within the well-established method of integral equations, the appearance of negative values of the static dielectric function (SDF) and the attraction of particles with charges of the same sign are demonstrated. In Sec. II, the solution of the Ornstein–Zernike equations in the hypernetted chain approximation is presented for a three-component Coulomb plasma, where the energies of electron–dust, ion–dust, electron–electron, electron–ion, and ion–ion interactions remain much smaller than their thermal energy. It is shown how the effective dust–dust Debye potential is formed. Furthermore, the conditions are determined for the dusty plasma static dielectric function to take negative values in the long wavelength domain, and the dust subsystem thermodynamic stability is studied. The preliminary short version of the present work was published in Ref. [36].

II. ORNSTEIN–ZERNIKE EQUATIONS FOR A MULTICOMPONENT PLASMA

We consider a three-component plasma with the interaction between charged particles described by the Coulomb potential,

$$V_{\nu\mu}(|\mathbf{r}_\nu - \mathbf{r}_\mu|) = \frac{e^2 z_\nu z_\mu}{|\mathbf{r}_\nu - \mathbf{r}_\mu|}. \tag{1}$$

Here, the Greek indices ν and μ take the value 0 for dust particles, 1 for electrons, and 2 for ions, z_ν is the charge number of ν-species particles, $z_1 = -1$, and $\mathbf{r}_\nu$ and $\mathbf{r}_\mu$ are the radius vectors to the positions of particles of ν and μ-species, respectively. Effective potentials are commonly introduced to eliminate problems with the electron–ion interaction and the interaction of dust particles with plasma particles with the charge of the opposite sign, to take into account quantum effects in the electron–electron interaction[37–42] (see also Refs. [32] and [33] and references therein) and to explicitly take into account the dust particle size.[31,43,44] At densities of the charged particles considered in this work, the plasma is far from degeneracy, and the interaction at small distances produces a negligible contribution, and therefore, the form of the potential at these distances and under these conditions is not significant.

The Ornstein–Zernike equation for a homogeneous multicomponent fluid has the form[23]

$$h_{\nu\mu}(r) = C_{\nu\mu}(r) + \sum_\lambda n_\lambda \int C_{\nu\lambda}(|\mathbf{r} - \mathbf{r}'|) h_{\lambda\mu}(r') d\mathbf{r}',$$
$$\nu = 0, 1, 2, \; \mu = 0, 1, 2, \tag{2}$$

where $h_{\nu\mu} = g_{\nu\mu} - 1$ and $C_{\nu\mu}$ are the partial and direct pair correlation functions, respectively; n_λ is the averaged number density of the λ-species particles,

$$n_\lambda = N_\lambda/V,$$

where N_λ is their total number in the system of the volume V. Therefore, the total quasineutrality condition takes the following form:

$$\sum_{\nu=0}^{2} z_\nu n_\nu = 0. \tag{3}$$

Given the symmetry of the correlation functions, that is, since $h_{\nu\mu} = h_{\mu\nu}$ and $C_{\nu\mu} = C_{\mu\nu}$, system (2) in the case of a three-component dusty plasma determines six correlation functions. The three-dimensional Fourier transformation converts this system of integral equations into the system of algebraic equations,

$$\widetilde{h}_{\nu\mu}(k) = \widetilde{C}_{\nu\mu}(k) + \sum_\lambda n_\lambda \widetilde{C}_{\nu\lambda}(k)\widetilde{h}_{\lambda\mu}(k). \tag{4}$$

Here and below, the Fourier transforms are marked with a tilde. From the equations for $\widetilde{h}_{01}$ and $\widetilde{h}_{02}$, their relationship with $\widetilde{h}_{00}$ can be found (note that Ref. [31] contains explicit expressions for similar correlation functions with some misprints),

$$\widetilde{h}_{01} = \left(1 + n_0\widetilde{h}_{00}\right)\frac{\widetilde{C}_{01}\left(1 - n_2\widetilde{C}_{22}\right) + n_2\widetilde{C}_{02}\widetilde{C}_{12}}{D(k)},$$
$$\widetilde{h}_{02} = \left(1 + n_0\widetilde{h}_{00}\right)\frac{\widetilde{C}_{02}\left(1 - n_1\widetilde{C}_{11}\right) + n_1\widetilde{C}_{01}\widetilde{C}_{12}}{D(k)}, \tag{5}$$

where

$$D(k) = \left(1 - n_1\widetilde{C}_{11}\right)\left(1 - n_2\widetilde{C}_{22}\right) - n_1 n_2\widetilde{C}_{12}^2.$$

Then, by substituting (5) into the equation for $\widetilde{h}_{00}$ in (4), the dust correlation function can be obtained,[29,31]

$$\widetilde{h}_{00}(k) = \widetilde{C}_{eff}(k) + n_0\widetilde{C}_{eff}(k)\widetilde{h}_{00}(k), \tag{6}$$

which involves the effective direct correlation function,

$$\widetilde{C}_{eff}(k) = \widetilde{C}_{00} + \frac{1}{D(k)}\Big[n_1\widetilde{C}_{01}^2\left(1 - n_2\widetilde{C}_{22}\right)$$
$$+ n_2\widetilde{C}_{02}^2\left(1 - n_1\widetilde{C}_{11}\right) + 2n_1 n_2\widetilde{C}_{01}\widetilde{C}_{02}\widetilde{C}_{12}\Big]. \tag{7}$$

One can see that Eq. (6) has the form of the OZ equation for a one-component liquid.

In this paper, conditions are considered when coupling is relevant only in the dust subsystem, i.e., only the interaction energy between dust particles can be much larger than their thermal energy. In addition, the energies of electron–dust, ion–dust, electron–electron, electron–ion, and ion–ion interactions remain much smaller than their thermal energy,

$$\Gamma_{01} = \frac{e^2 z_0 n_0^{1/3}}{T_0} \ll 1, \; \Gamma_{02} = \frac{e^2 z_2 z_0 n_0^{1/3}}{T_0} \ll 1,$$
$$\Gamma_{11} = \frac{e^2 n_1^{1/3}}{T_1} \ll 1, \tag{8}$$
$$\Gamma_{12} = \frac{e^2 z_2 n_2^{1/3}}{T_2} \ll 1, \; \Gamma_{22} = \frac{e^2 z_2^2 n_2^{1/3}}{T_2} \ll 1,$$

where T_1 and T_2 are electron and ion temperatures in energy units, respectively. In what follows, an isothermal plasma is considered with $T_0 = T_1 = T_2 \equiv T$, but the results, with some restrictions, can also be used to describe nonisothermal and nonequilibrium systems (see Ref. 45 and the literature cited therein).

Under conditions (8), it is possible to approximate the direct correlation functions by the following expressions[23] ($\nu = 0, 1, 2$; $\mu = 1, 2$):

$$C_{\nu\mu}(r) = -\beta V_{\nu\mu}(r) \equiv -\frac{e^2 z_\nu z_\mu \beta}{r}, \qquad (9)$$

with the Fourier transforms

$$\widetilde{C}_{\nu\mu}(k) = -\frac{4\pi e^2 z_\nu z_\mu \beta}{k^2}, \quad \nu = 0, 1, 2; \mu = 1, 2. \qquad (10)$$

Here, β is the inverse temperature: $\beta = 1/T$. Using (10), from Eq. (5), one finds that

$$\widetilde{h}_{01}(k) = 4\pi e^2 z_0 \beta \frac{1 + n_0 \widetilde{h}_{00}(k)}{k^2 + k_{ei}^2},$$
$$\widetilde{h}_{02}(k) = -4\pi e^2 z_0 z_2 \beta \frac{1 + n_0 \widetilde{h}_{00}(k)}{k^2 + k_{ei}^2}, \qquad (11)$$

where $k_{ei}^2 = k_1^2 + k_2^2$, with the electron, k_1, and ion, k_2, screening constants defined by relations

$$k_1^2 = 4\pi e^2 n_1 \beta, \quad k_2^2 = 4\pi e^2 z_2^2 n_2 \beta. \qquad (12)$$

Note that $\widetilde{h}_{01}\widetilde{C}_{02} = \widetilde{h}_{02}\widetilde{C}_{01}$ and $z_1 \widetilde{h}_{02} = z_2 \widetilde{h}_{01}$. Similarly, from Eq. (7),

$$\widetilde{C}_{eff}(k) = \widetilde{C}_{00}(k) + \frac{4\pi e^2 z_0^2 \beta k_{ei}^2}{k^2 (k^2 + k_{ei}^2)}, \qquad (13)$$

and after the inverse Fourier transform, it follows from Eq. (13) that

$$C_{eff}(r) = C_{00}(r) + \frac{e^2 z_0^2 \beta}{r}\left(1 - e^{-k_{ei} r}\right). \qquad (14)$$

Furthermore, Eq. (2) is closed by the relation

$$h_{\nu\mu}(r) = e^{-\beta V_{\nu\mu}(r) + h_{\nu\mu}(r) - C_{\nu\mu}(r) + B_{\nu\mu}(r)} - 1, \qquad (15)$$

where $B_{\nu\mu}(r)$ is the bridge functional.[24] Finally, the expression for h_{00} can be written explicitly as

$$h_{00}(r) = \exp\left[-\frac{e^2 z_0^2 \beta}{r} e^{-k_{ei}r} + h_{00}(r) - C_{eff}(r) + B_{00}(r)\right] - 1. \qquad (16)$$

This result implies that the solution for h_{00} will not change if the effective Debye potential

$$V_{eff}(r) = \frac{e^2 z_0^2}{r} e^{-k_{ei}r} \qquad (17)$$

is introduced. It is important that the screening constant in this case is determined only by electrons and ions whose number densities are related to that of the dust particles by the total quasineutrality condition (3). Therefore, when the charge or number density of dust particles varies, the screening constant k_{ei} also changes.

In the HNC approximation, the bridge functional is assumed to be zero: $B_{\nu\mu}(r) = 0$ and for the closure of the OZ Eq. (6), the equation

$$h_{00}(\mathbf{r}) = e^{-\beta V_{eff}(\mathbf{r}) + h_{00}(\mathbf{r}) - C_{eff}(\mathbf{r})} - 1 \qquad (18)$$

can be employed. From the last three equations of system (4), one can determine the Fourier transforms of the remaining pair correlation functions,

$$\widetilde{h}_{11} = \frac{\widetilde{C}_{11} + n_0 \widetilde{C}_{10}\widetilde{h}_{01}}{D(k)}, \quad \widetilde{h}_{12} = \frac{\widetilde{C}_{12} + n_0 \widetilde{C}_{10}\widetilde{h}_{02}}{D(k)},$$
$$\widetilde{h}_{22} = \frac{\widetilde{C}_{22} + n_0 \widetilde{C}_{20}\widetilde{h}_{02}}{D(k)}. \qquad (19)$$

We emphasize here that the effective potential V_{eff} is introduced only to separate from the system of OZ Eq. (4) an OZ equation for h_{00}, which can be solved by standard numerical methods if direct correlation functions $C_{\nu\mu}$ for $\nu = 0, 1, 2$ and $\mu = 1, 2$ are known. The pair interaction potential of charged particles in the plasma remains the Coulomb one. In general, V_{eff} is defined by the expression

$$V_{eff}(r) = V_{00} - \frac{1}{2\pi^2 \beta r} \int_0^\infty \frac{1}{D(k)}\left[n_1 \widetilde{C}_{01}^2\left(1 - n_2 \widetilde{C}_{22}\right) + n_2 \widetilde{C}_{02}^2\left(1 - n_1 \widetilde{C}_{11}\right) + 2n_1 n_2 \widetilde{C}_{01}\widetilde{C}_{02}\widetilde{C}_{12}\right] k \sin(kr)\, dk. \qquad (20)$$

Under conditions (8) for the direct correlation functions, one can use Eqs. (9) and (20), which lead to the Debye potential (17). Equation (20) can be employed to solve the system of OZ equations for a multicomponent system by the iteration method, in which the OZ equation for the subsystem with the strongest interaction is solved separately from the other five equations. In this case, direct correlation functions (9) can be used as initial solutions.

III. STATIC DIELECTRIC FUNCTION OF A MULTICOMPONENT DUSTY PLASMA

In a classical system, the static dielectric function (SDF) is determined by the charge response function χ_{ZZ}, which itself is connected to the structure factor by the fluctuation–dissipation theorem,[23,46,47]

$$\chi_{ZZ}(k) \equiv \sum_\nu \sum_\mu z_\nu z_\mu \chi_{\nu\mu}(k) = -\beta n S_{ZZ}(k). \qquad (21)$$

Here, $\chi_{\nu\mu}$ is the partial response function directly related to the partial structure factor,[23]

$$\chi_{\nu\mu}(k) = -\beta n S_{\nu\mu}(k), \qquad (22)$$

where n is the total number density of plasma charged particles: $n = \sum_\nu n_\nu$; $S_{ZZ}(k)$ is the charge–charge structure factor,

$$S_{ZZ}(k) = \sum_\nu \sum_\mu z_\nu z_\mu S_{\nu\mu}(k), \qquad (23)$$

where $S_{\nu\mu}(k)$ are the partial structure factors,[23]

$$S_{\nu\mu}(k) = \frac{n_\nu}{n}\left[\delta_{\nu\mu} + n_\mu \widetilde{h}_{\nu\mu}(k)\right], \qquad (24)$$

where $\delta_{\nu\mu}$ is the Kronecker delta. Therefore, for the inverse SDF, one has

$$\frac{1}{\varepsilon(k)} = 1 + \frac{4\pi e^2}{k^2} \chi_{ZZ}(k) \equiv 1 - \frac{4\pi e^2}{k^2} \beta n S_{ZZ}(k). \qquad (25)$$

The charge–charge static structure factor $S_{ZZ}(k)$ is, by definition, the average square of the charge fluctuations, then, it is non-negative.[48] Therefore, the following inequality stems from (25),

$$\frac{1}{\varepsilon(k)} \leq 1, \tag{26}$$

which is valid for all wavenumber values. This inequality allows for negative values both of the inverse SDF and the SDF itself, which cannot take values in the range from zero to one: $\varepsilon(k) \geq 1$ or $\varepsilon(k) < 0$.[49,50]

Thus, the expression for the inverse SDF, (25), due to conditions (8) and by virtue of (11) and (19), can be rewritten as

$$\frac{1}{\varepsilon(k)} = 1 - \frac{k_D^2}{k^2} + \frac{k_{ei}^4}{k^2}\frac{1 - k_0^2 f(k)}{k^2 + k_{ei}^2} - \frac{k_0^2}{k^2}n_0\widetilde{h}_{00}(k) + \frac{2k_0^2 k_{ei}^2}{k^2}f(k), \tag{27}$$

where k_0 is the screening constant of the dust component: $k_0^2 = 4\pi e^2 z_0^2 n_0 \beta$; k_D is the full screening constant,

$$k_D^2 = \sum_{\nu=0,1,2} k_\nu^2 = \sum_{\nu=0,1,2} 4\pi\beta e^2 z_\nu^2 n_\nu, \tag{28}$$

and $f(k)$ is the following auxiliary function:

$$f(k) = \frac{1 + n_0\widetilde{h}_{00}(k)}{k^2 + k_{ei}^2}. \tag{29}$$

IV. INTERACTION POTENTIAL BETWEEN CHARGED PARTICLES

The potential of a point charge q located at point $\mathbf{r}_0$ in the coordinate space is determined by the following expression:[51]

$$\varphi(\mathbf{r}) = \frac{q}{(2\pi)^3}\int \frac{e^{i\mathbf{k}(\mathbf{r}-\mathbf{r}_0)}}{\varepsilon(k)}\frac{4\pi}{k^2}d\mathbf{k}, \tag{30}$$

or by placing a charge at the origin of the coordinate system $\mathbf{r}_0 = 0$,

$$\varphi(r) = \frac{2q}{\pi r}\int_0^\infty \frac{\sin(kr)}{k\varepsilon(k)}dk. \tag{31}$$

Therefore, the interaction potential of two point charges q_1 and q_2 located at a distance R from each other is determined by the following expression:

$$U(R) = \frac{2q_1 q_2}{\pi R}\int_0^\infty \frac{\sin(kR)}{k\varepsilon(k)}dk. \tag{32}$$

Note that Eq. (32) describes the interaction of external test particles, and the interaction potential of internal charges may differ from this one, but if the interaction is weak, this difference can be neglected (see in detail in Ref. 52, p.53).

V. PRESSURE AND INTERNAL ENERGY

The interaction-associated part of the internal energy in a homogeneous plasma is defined as[23]

$$\Delta U = \frac{1}{2}\sum_\nu \sum_\mu n_\nu n_\mu \int V_{\nu\mu}(r)g_{\nu\mu}(r)d\mathbf{r}, \tag{33}$$

and the pressure as[23]

$$P = \frac{n}{\beta} - \frac{1}{6}\sum_\nu \sum_\mu n_\nu n_\mu \int \mathbf{r}\frac{\partial V_{\nu\mu}(r)}{\partial \mathbf{r}}g_{\nu\mu}(r)d\mathbf{r}. \tag{34}$$

Hence, for the Coulomb interaction potential (1), taking into account the condition of total quasineutrality (3), one finds

$$\Delta U = 2\pi e^2 \sum_\nu \sum_\mu n_\nu n_\mu z_\nu z_\mu \int_0^\infty h_{\nu\mu}(r)rdr, \tag{35}$$

$$P = \frac{n}{\beta} + \frac{2\pi e^2}{3}\sum_\nu \sum_\mu n_\nu n_\mu z_\nu z_\mu \int_0^\infty h_{\nu\mu}(r)rdr = \frac{n}{\beta} + \frac{1}{3}\Delta U. \tag{36}$$

VI. DEBYE APPROXIMATION

In this section, the case is considered when the dust subsystem is also ideal, i.e., the Debye approximation is also applicable to the dust component,

$$\Gamma_{00} = \frac{e^2 z_0^2 n_0^{1/3}}{aT} \ll 1, \tag{37}$$

where a is the average interparticle distance for the dusty subsystem: $a = n_0^{-1/3}$. In this case, it stems from (13) that

$$\widetilde{C}_{eff}(k) = -\frac{4\pi e^2 z_0^2 \beta}{k^2 + k_{ei}^2}, \tag{38}$$

and, from (6), one obtains

$$\widetilde{h}_{00}(k) = -\frac{4\pi e^2 z_0^2 \beta}{k^2 + k_D^2}. \tag{39}$$

Furthermore, from (11) and (19), the pair correlation function takes the following simple form valid for all ν and μ:

$$\widetilde{h}_{\nu\mu}(k) = -\frac{4\pi e^2 z_\nu z_\mu \beta}{k^2 + k_D^2}. \tag{40}$$

Then, by performing the inverse Fourier transform, the well-known result[47] is recovered,

$$g_{\nu\mu}(r) = 1 - \frac{e^2 z_\nu z_\mu \beta}{r}e^{-k_D r}. \tag{41}$$

Furthermore, other expected results follow, using (41), from (25) for the static dielectric function,

$$\frac{1}{\varepsilon(k)} = 1 - \frac{k_D^2}{k^2 + k_D^2}, \quad \varepsilon(k) = 1 + \frac{k_D^2}{k^2}. \tag{42}$$

With the Debye SDF (42), from Eq. (32), one shows that, in the case of ideality of all subsystems of the dusty plasma, the interaction potential of point charges in such a system will be the Debye one with the full screening constant,

$$U_D(r) = \frac{2q_1 q_2}{\pi R}\int_0^\infty \frac{k\sin(kR)}{k^2 + k_D^2}dk = \frac{q_1 q_2}{R}e^{-k_D R}. \tag{43}$$

Hence, using (41), the well-known relations[47] follow for the internal energy and pressure from (35) and (36),

$$\Delta U = -2\pi e^4 \sum_{\nu} \sum_{\mu} n_{\nu} n_{\mu} z_{\nu}^2 z_{\mu}^2 \frac{\beta}{k_D}$$

$$= -\frac{e^2}{2k_D} \sum_{\nu} \sum_{\mu} n_{\nu} z_{\nu}^2 k_{\mu}^2$$

$$= -\frac{e^2 k_D}{2} \sum_{\nu} n_{\nu} z_{\nu}^2, \tag{44}$$

$$P = \frac{n}{\beta} - \frac{e^3}{3} \sqrt{\frac{\pi}{T}} \left(\sum_{\nu} n_{\nu} z_{\nu}^2 \right)^{3/2}. \tag{45}$$

VII. NUMERICAL SIMULATIONS AND DISCUSSION OF RESULTS

Next, our results of a numerical study of the electrostatic interaction in the dusty plasma are presented based on the numerical solution of the OZ Eq. (6) in the HNC approximation (18) and on the basis of the molecular dynamics (MD) method with potential (17). Note that the hypernetted-chain approximation is applied to the strongly coupled dusty subsystem only. The iterative method for solving the OZ equation in the HNC approximation is described in detail in Ref. 25. At the zeroth iteration, the structure factors in the Debye approximation (40) are used. To speed up the convergence, the procedure proposed in Ref. 53 is applied. In order to calculate integrals that converge poorly or have removable singularities at small wavenumbers, for example, to calculate the potential (31), we used the standard procedure of extraction of the long-range Debye asymptotes or singularities, the integral of which can be calculated analytically, and numerically integrating the remainder.

In the calculations, the ion number density was fixed as $n_2 = 10^8$ cm^{-3}, their charge number $z_2 = 1$, the number density of dust particles $n_0 = 10^5$ cm^{-3}, and the temperature $\overline{T} = 300$ K ($\overline{T}$ is

the temperature in kelvins: $\overline{T} = T/k_B$, k_B is the Boltzmann constant). The coupling parameter Γ (hereinafter, Γ means Γ_{00}) was varied by changing the negative charge of dust particles z_0, and the electron number density was determined from the condition of total quasineutrality (3). Therefore, the electron number density and, accordingly, the electron and electron–ion screening constants decreased with increasing Γ, and the full screening constant increased.

Table I shows the characteristic values of the coupling parameters and screening constants for a number of dust particle charges (in elementary charges) at a fixed ion number density $n_2 = 10^8$ cm^{-3}, $z_2 = 1$, and the room temperature $\overline{T} = 300$ K. It can be seen that up to $z_0 = -10^3$, the values of all coupling parameters, except for Γ_{00}, are noticeably smaller than unity.

Our results for the structure factor of the dust component found from the OZ equation in the HNC approximation for different coupling parameter values are presented in Fig. 1. Here, the structure factor of the dust component is defined as

$$S(k) = 1 + n_0 \widetilde{h}_{00}(k), \tag{46}$$

that is, without the factor n_0/n in the partial structure factor (24). One can see how, with increasing Γ, the values of the structure factor decrease for small values of wavenumber k, while the number of peaks and their amplitudes grow.

Figure 2 shows both the inverse and direct static dielectric functions of the dusty plasma obtained according to Eq. (27) from the OZ equation in the HNC approximation. It can be seen that for $\Gamma \leq 1$, the SDF is positive, and for $\Gamma = 3.2$ in the region of small wavenumber values, it is negative. As the value of the coupling parameter increases, the region of negative values moves further into the region of large values of k, and the absolute values of the SDF grow. The possibility of the appearance of negative SDF values was discussed in Refs. 28, 54, and 55. The data on $\varepsilon(k)$ presented in Refs. 28 and 55 are similar to the ones shown in Fig. 2, but nevertheless do differ from them since in those works, as in Ref. 54, the scheme for determining the SDF was not entirely consistent. For example, in Ref. 55, the SDF of a one-component plasma (OCP) was determined from

TABLE I. Coupling parameters and screening constants for a series of dust particle charges (in elementary charges) in the dusty plasma at $n_0 = 10^5$ cm^{-3}, $n_2 = 10^8$ cm^{-3}, $z_2 = 1$, and $\overline{T} = 300$ K.

| z_0	-1	-10	-100	-1000
n_e, cm^{-3}	9.99×10^7	9.9×10^7	9.0×10^7	0.0
Γ_{00}	2.58×10^{-4}	2.58×10^{-2}	2.58	2.58×10^2
Γ_{01}	2.58×10^{-4}	2.58×10^{-3}	2.58×10^{-2}	2.58×10^{-1}
Γ_{02}	2.58×10^{-4}	2.58×10^{-3}	2.58×10^{-2}	2.58×10^{-1}
Γ_{11}	2.58×10^{-3}	2.57×10^{-3}	2.49×10^{-3}	0.0
Γ_{12}	2.58×10^{-3}	2.58×10^{-3}	2.58×10^{-3}	2.58×10^{-3}
Γ_{22}	2.58×10^{-3}	2.58×10^{-3}	2.58×10^{-3}	2.58×10^{-3}
k_0 (cm^{-1})	2.6	26.4	264.5	2644.5
k_1 (cm^{-1})	83.6	83.2	79.3	0.0
k_2 (cm^{-1})	83.6	83.6	83.6	83.6
k_{ei} (cm^{-1})	118.2	118.0	115.3	83.6
k_D (cm^{-1})	118.3	120.9	288.5	2645.8
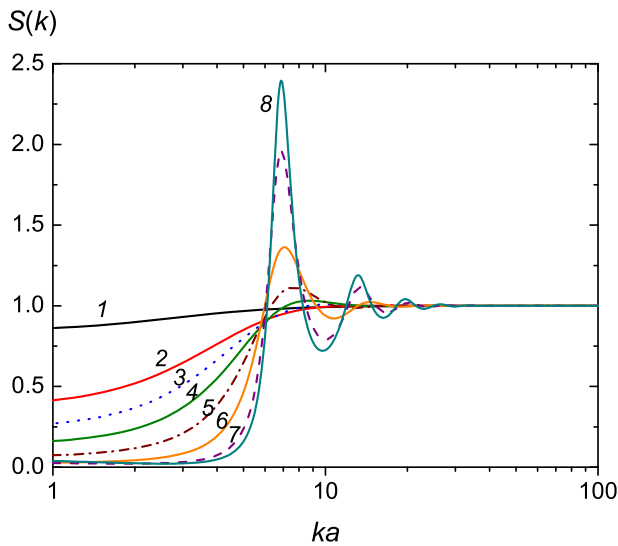
FIG. 1. The structure factor of the dust component found from the OZ equation in the HNC approximation for different coupling parameter values: curve 1 corresponds to $\Gamma = 0.1$, and curves 2, 3, 4, 5, 6, 7, and 8 correspond, respectively, to $\Gamma = 1, 2, 4, 10, 30, 100$, and 155.

the expression (in the notation of the present paper)

$$\varepsilon(k) = \frac{k^2}{k^2 - k_0^2 S(k)}, \quad (47)$$

where $S(k)$ is defined as in (46) but with $\widetilde{h}_{00}(k)$ found for the Coulomb interaction potential between dust particles with the charge z_0. Notice that Eq. (27) cannot be reduced to a simple expression (47) containing only k_0 and $\widetilde{h}_{00}$. Moreover, for small values of the coupling parameter in the Debye approximation (39) (with k_D replaced by k_0), Eq. (47) becomes the Debye approximation expression (42).

Figure 2 also shows $\varepsilon^{-1}(k)$ and $\varepsilon(k)$ for $\Gamma = 1, 5, 10$, and 100, all obtained on the basis of calculations of the structure factor of dust particles by the method of molecular dynamics (MD) with the potential (17). For all partial structure factors, except for S_{00}, the Debye approximation was used, and the structure factor of the dust subsystem was calculated by the MD method using the following algorithm. First, the radial distribution function $g_{00}(r)$ was calculated, and the cutoff radius was taken to be equal to $r_{cut} = 13a$ (see Refs. 25 and 26). The values of the function $g_{00}(r)$ were averaged over time with 1000 values corresponding to different times taken into account. In addition, averaging was performed according to the results of five independent calculations. Then, the structure factor was calculated by formula (24). Replacing the infinite limit of integration with a finite one under the Fourier transform inevitably leads to an error, which becomes especially significant for small k. Therefore, in this paper, the values of $S_{00}(k)$ were calculated only for $ka > 1$. An increase in the limiting radius to $r_{cut} = 18a$ did not lead to a noticeable change in $S_{00}(k)$ in the selected range of k values. Figure 2 confirms a very good agreement between the data obtained by two different methods, and the discrepancy for small k for $\Gamma = 100$

(a)

(b)
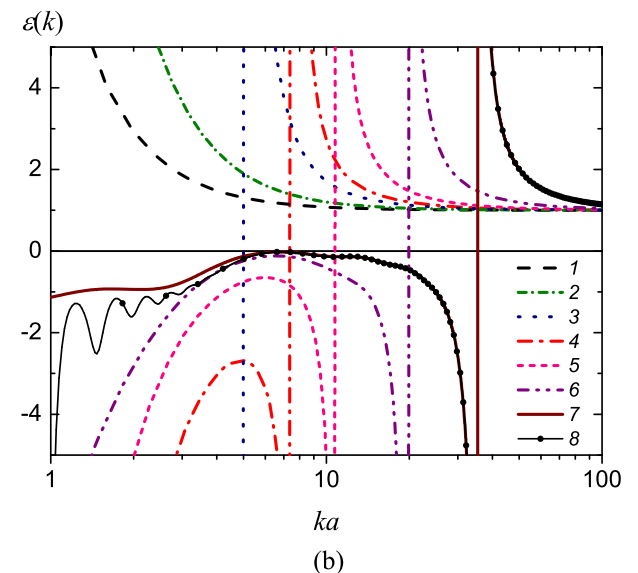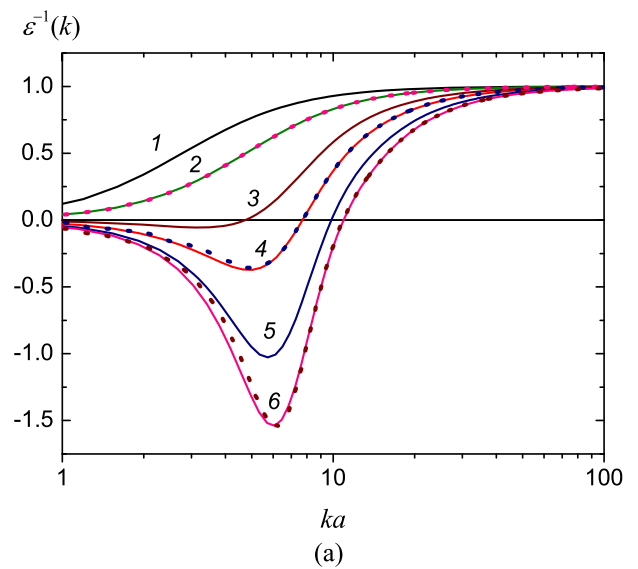
FIG. 2. The dusty plasma inverse (a) and direct SDF (b) for the following coupling parameter values: 1—$\Gamma = 0.1$, 2—$\Gamma = 1$, 3—$\Gamma = 3.2$, 4—$\Gamma = 5$, 5—$\Gamma = 7.9$ (a) or 10 (b), 6—$\Gamma = 10$ (a) or 32 (b), and 7 and 8—$\Gamma = 100$ (b); (a) solid lines were obtained by solving the OZ equation in the HNC approximation, and dotted lines represent our results of simulation by the MD method for $\Gamma = 1, 5$, and 10; (b) curves 1–7 show solutions of the OZ equation in the HNC approximation, and 8 displays the results of the MD method simulations.

reflects the noted difficulty in determining the structure factor by the MD method of the molecular dynamics in this domain.

The dust interaction potential determined from Eqs. (32) and (43) is displayed in Fig. 3. It can be seen that for $\Gamma < 1$, it is described by the Debye potential quite well. At $\Gamma = 1$ at distances larger than the Debye radius, deviations from the Debye behavior are visible. With a further increase in the coupling parameter, a region of interparticle distances appears, where attraction is observed between particles
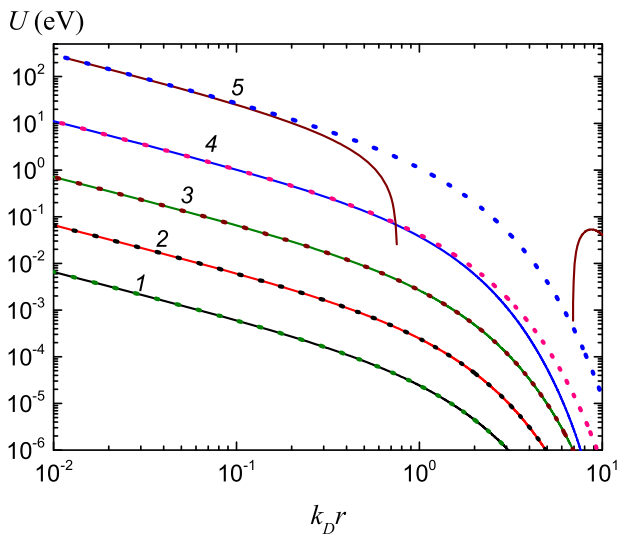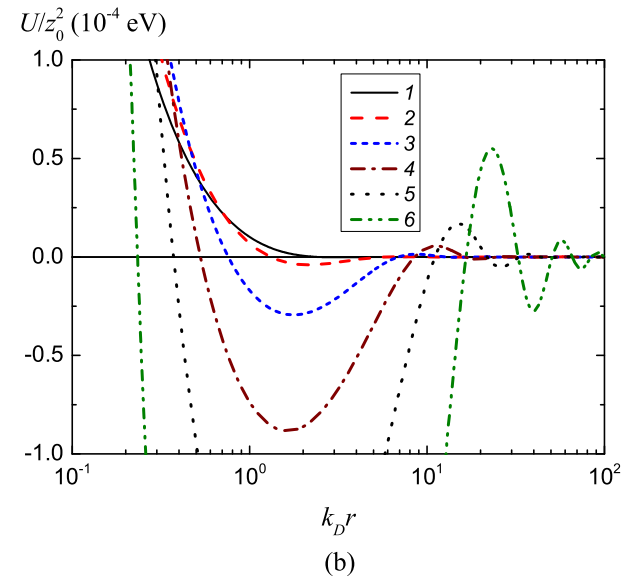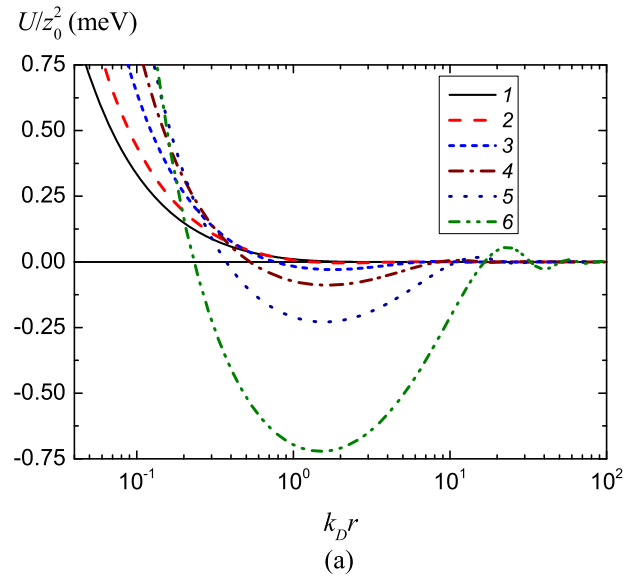
FIG. 3. The interaction potential of dust particles at low values of the coupling parameter, curves 1, 2, 3, 4, and 5 correspond to the values of $\Gamma = 10^{-3}$, 10^{-2}, 10^{-1}, 1, and 10, respectively. The solid curves are based on the solution of the OZ equation in the HNC approximation, as in Eq. (32); the dotted ones are the Debye potential (43).

with charges of the same sign, which is well illustrated in Fig. 4. It is seen that with increasing Γ, the attraction region expands, the well depth grows, a barrier appears in the interaction potential from the side of large distances, and the potential takes on an oscillating character.

Figure 5 shows the Debye form (43) of the interaction potential of dust particles, which indicates that for small values of the coupling parameter $\Gamma < 10^{-1}$ (with $z_0 < 20$), deviation from the Debye theory is insignificant. With an increase in Γ, the deviations are more visible, and already at $\Gamma \simeq 1$ an attraction appears between particles of the same charge sign at large distances among them. Note here that the approach with a dielectric function responsible for the interaction screening corresponds to the continuous medium picture and reflects a statistically averaged setting of the interaction. Therefore, it is applicable only at distances much larger than the average interparticle distance: $r \gg a$, and at smaller distances, fluctuations in the position of individual particles must be accounted for. In the negative interaction potential interval of distances at $\Gamma \simeq 1$, as it can be seen from Fig. 5, this applicability condition is satisfied, and the formation of a potential trap and barriers at $\Gamma \geq 2$ require further investigation.

Both left-hand and right-hand boundaries of the above negative interaction interval (before the first maximum) are displayed in Fig. 6. It is clearly seen that the left-hand boundary with the growth of the coupling parameter Γ moves further and further to smaller distances, and the right-hand boundary moves to larger distances. Note that, for $\Gamma < 2$, the right-hand boundary was not determined because of the weakness of the interaction in this region. From Fig. 6, it can be seen that negative potential values appear already at $\Gamma \sim 0.5$, but this only takes place at distances exceeding 20 D radii, so it unlikely has any physical value. At $\Gamma \geq 1$, the interaction potential


(a)

(b)

FIG. 4. Graphs of the dust particle interaction potential vs $k_D r$ for $\Gamma > 1$ with large (a) and small scales along the ordinate axis (b): 1—$\Gamma = 2$, 2—$\Gamma = 4$, 3—$\Gamma = 10$, 4—$\Gamma = 20$, 5—$\Gamma = 40$, and 6—$\Gamma = 100$.

changes its sign at distances of several Debye radii and less, which will play an important role in dusty plasmas, especially in the processes of formation of ordered dusty plasma structures and phase transitions.

Figure 6 also shows the points of the first (from the side of small distances) minimum and maximum of the interaction potential between dust particles, and Fig. 7 shows the potential values at these points. For $\Gamma < 2$, the maximum points were not determined for the same reason as the right-hand boundaries on Fig. 6. From Figs. 6 and 7, it can be concluded that the interparticle distance at which the
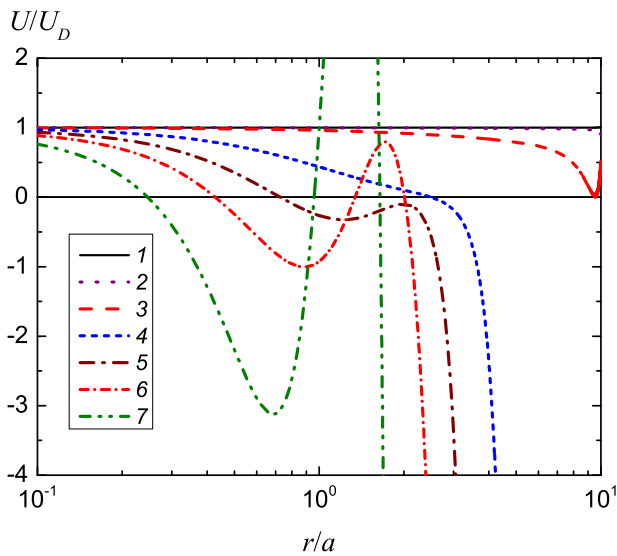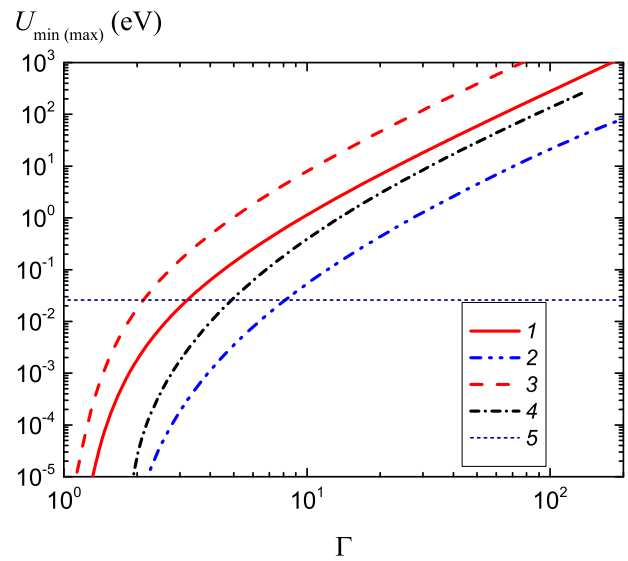
FIG. 5. Interaction potential of dust particles reduced to the Debye one for small values of the coupling parameter: 1—$\Gamma = 10^{-2}$, 2—$\Gamma = 10^{-1}$, 3—$\Gamma = 0.32$, 4—$\Gamma = 1$, 5—$\Gamma = 1.5$, 6—$\Gamma = 2$, and 7—$\Gamma = 3$.

interaction between dust particles passes from repulsion to attraction (the point of the potential minimum) decreases with increasing Γ and is about 1.5 D radius at high values of the coupling parameter. In addition, at $\Gamma > 3$, the depth of the well noticeably exceeds the thermal energy of dust particles.
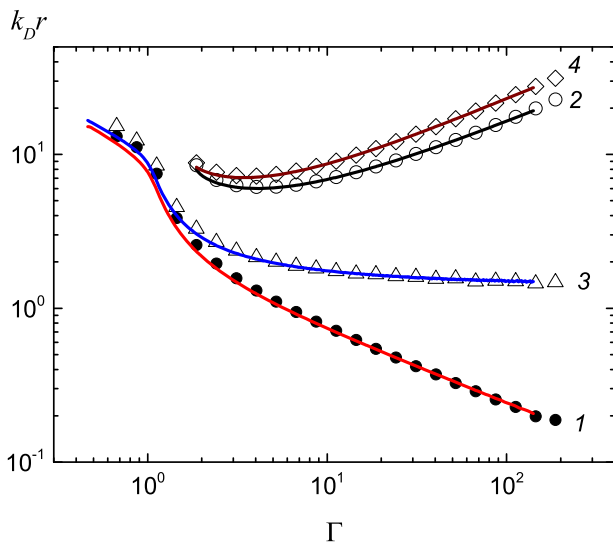
FIG. 6. Left-hand (curve 1) and right-hand (2) boundaries of negative values (before the first maximum), positions of the first minimum (3) and maximum (4) of the dust particle interaction potential found from the solution of the OZ equation in the HNC approximation vs the coupling parameter Γ. Symbols are for $n_0 = 10^5$ cm^{-3}, $n_2 = 10^8$ cm^{-3}, $\overline{T} = 300$ K, and $z_0 < 0$; solid curves are for $n_0 = 10^7$ cm^{-3}, $n_2 = 10^{10}$ cm^{-3}, $\overline{T} = 2000$ K, and $z_0 > 0$.

FIG. 7. The values of the interaction potential of dust particles at the point of the first minimum ($-U_{min}$, curves 1 and 3) and the first maximum (U_{max}, curves 2 and 4) obtained from the solution of the OZ equation in the HNC approximation vs the coupling parameter Γ. Curves 1 and 2 are for $n_0 = 10^5$ cm^{-3}, $n_2 = 10^8$ cm^{-3}, $\overline{T} = 300$ K, and $z_0 < 0$; 3 and 4 for $n_0 = 10^7$ cm^{-3}, $n_2 = 10^{10}$ cm^{-3}, $\overline{T} = 2000$ K, and $z_0 > 0$. Curve 5 corresponds to the room temperature value in energy units: $T = 0.0259$ eV.

The approach used in the present work deals with plasmas in thermal equilibrium, although it is possible to use expressions for direct correlation functions (9) obtained on the basis of the Bogoliubov–Born–Green–Kirkwood–Yvon (BBGKY) hierarchy for a nonisothermal plasma under conditions (8). This approach without restrictions is applicable for thermal dusty plasma, which was the case, for example, in Refs. 56–58. Here, we calculated the dielectric properties and the interaction potential in a dusty plasma in thermal equilibrium and with the following parameters close to the experimental ones:[56–58] $n_0 = 10^7$ cm^{-3}, $n_2 = 10^{10}$ cm^{-3}, and $\overline{T} = 2000$ K, and it was assumed that the charge of dust particles due to the thermal emission of electrons is positive: $z_0 > 0$. Notice that the addition of alkali metal atoms, which are contained in small amounts in air, can influence the number density of ions and electrons significantly, and the charge of dust particles can be changed by changing their size or using materials with a different electron-work function.

Our calculations showed that negative values of SDF and the attraction of likely charged particles take place in dusty plasmas in thermal equilibrium at $\Gamma \gtrsim 1$ also. Both left-hand and right-hand boundaries of the region of negative values, as well as the positions of the first minimum and maximum of the interaction potential of dust particles in such a plasma are presented in Fig. 6 as well. It can be seen that the picture is very similar to the case of a plasma with negative charges. Figure 7 shows the values of the interaction potential at the minimum of the potential trap and at the point of the first maximum in a dusty plasma in thermal equilibrium. It can be seen that in this case, both the depth of the potential well and the height of the barrier turn out to be higher than in the plasma with negative

charges, but otherwise, their dependence on the coupling parameter is similar. With a decrease in the ion number density to 10^9 cm^{-3}, noticeable changes in the above picture were not observed.

The appearance of negative values of the static dielectric function[49,50] indicates the instability of the system and the possibility of a transition to a new phase. Earlier, in Refs. 59 and 60, for degenerate plasmas, a plasma phase transition was predicted at $\Gamma \gtrsim 1$. Then, both in the one-component approximation[28,55] and by extrapolating the results of the Debye theory, it was shown that the system loses its stability at $\Gamma \simeq 3$, which is consistent with the results obtained in the present paper.

Interaction corrections were estimated to the pressure of a dusty plasma with both negative and positive charges of dust particles, see Fig. 8. Observe that for $\Gamma < 1$, the pressure correction is small and is well described by the Debye theory. As Γ increases, the pressure correction increases, but the total pressure remains positive in the entire range of variation of the coupling parameter studied in this paper.

It follows from Fig. 8 that with increasing Γ, the discrepancy between the data obtained on the basis of the numerical solution of the OZ equation in the HNC approximation and within the Debye approximation grows. Furthermore, the results obtained in the framework of the Debye theory, i.e., in the Debye approximation for all subsystems, will be referred to as those obtained in the Debye approximation. Note that in the Debye approximation, the absolute value of the pressure correction reduced to n/β in the case of $z_0 < 0$ overcomes the unity for $\Gamma > 160$, i.e., then, the total pressure becomes negative. For $z_0 > 0$, in dusty plasmas in thermal equilibrium, $|\Delta P/nT|$ remains smaller than unity up to $\Gamma = 290$. In other words, in the range of variation of the coupling parameter of dusty plasmas in thermal equilibrium investigated in this work, the total pressure remains positive in the Debye approximation as well.

Taking into account that for high coupling parameter values, $n_0 z_0^2 \gg n_1 z_1^2 + n_2 z_2^2$, from (45) for the value of the coupling parameter $\Gamma_{00,n}$, above which the total pressure becomes negative, we have an estimate

$$\Gamma_{00,n} \approx \left(\frac{3n}{\sqrt{\pi}n_0}\right)^{2/3}. \qquad (48)$$

Hence, for the dust plasma parameters considered here for $z_0 < 0$, since large values of the coupling parameter $n \approx n_2$, $\Gamma_{00,n} = 142$, and for $z_0 > 0$, taking into account that for large Γ, we have $n \approx 3n_2$ and $\Gamma_{00,n} = 295$. These values explain the observed pressure behavior in the Debye approximation.

The partial corrections to the pressure $\Delta P_{\nu\mu}$ defined as

$$\Delta P_{\nu\mu} = \frac{2\pi e^2}{3} n_\nu n_\mu z_\nu z_\mu \int_0^\infty h_{\nu\mu}(r) r dr \qquad (49)$$

are presented in Fig. 9. Notice that the main contribution to the full correction comes from the interaction of dust particles with each other, a smaller contribution corresponds to their interaction with ions and even smaller to that with electrons. The most interesting feature is that the corrections due to the electron–electron, electron–ion, and ion–ion interactions are negative for small Γ and become positive with increasing Γ. From Fig. 9, it can be seen that these corrections do not exceed 1% of ΔP_{00}.

It stems also from Fig. 10 that for small Γ, the partial corrections to the pressure coincide with the partial corrections to the pressure in the Debye approximation,

$$\Delta P_{\nu\mu}^D = -\frac{2\pi e^4}{3} n_\nu n_\mu z_\nu^2 z_\mu^2 \frac{\beta}{k_D} = -\frac{e^2}{6k_D} n_\nu z_\nu^2 k_\mu^2. \qquad (50)$$
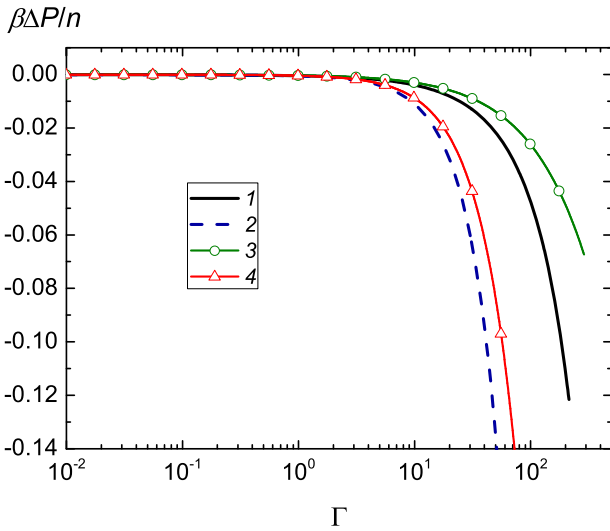
FIG. 8. Pressure corrections due to the Coulomb interaction in a multicomponent dusty plasma vs the coupling parameter. Curves 1 and 2 are for $n_0 = 10^5$ cm^{-3}, $n_2 = 10^8$ cm^{-3}, $\overline{T} = 300$ K, and $z_0 < 0$; 3 and 4 are for $n_0 = 10^7$ cm^{-3}, $n_2 = 10^{10}$ cm^{-3}, $\overline{T} = 2000$ K, and $z_0 > 0$. Curves 1 and 3 are the pressure corrections (36) obtained by the numerical solution of the OZ equation in the HNC approximation, and curves 2 and 4 are the pressure corrections within the Debye approximation (45).
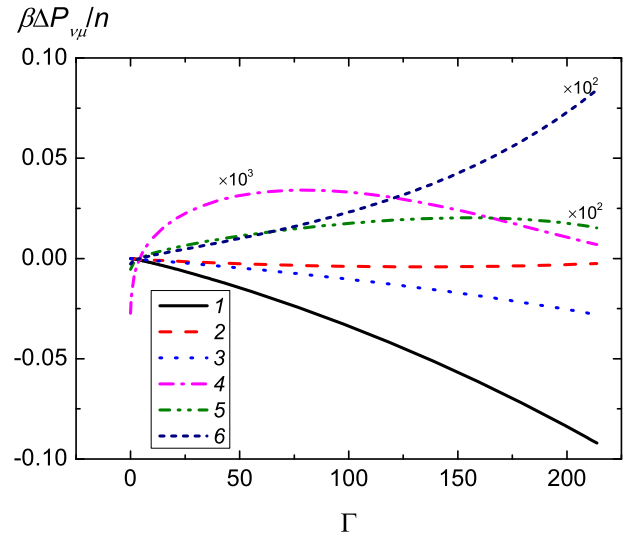
FIG. 9. Partial corrections to the pressure due to the Coulomb interaction in a multicomponent dusty plasma vs the coupling parameter for $n_0 = 10^5$ cm^{-3}, $n_2 = 10^8$ cm^{-3}, $\overline{T} = 300$ K, and $z_0 < 0$, found on the basis of the solution of the OZ equation in the HNC approximation [separate summands in (45)]. Curves 1, 2, 3, 4, 5, and 6 display, respectively, P_{00}, $2P_{01}$, $2P_{02}$, P_{11}, $2P_{12}$, and P_{22}.
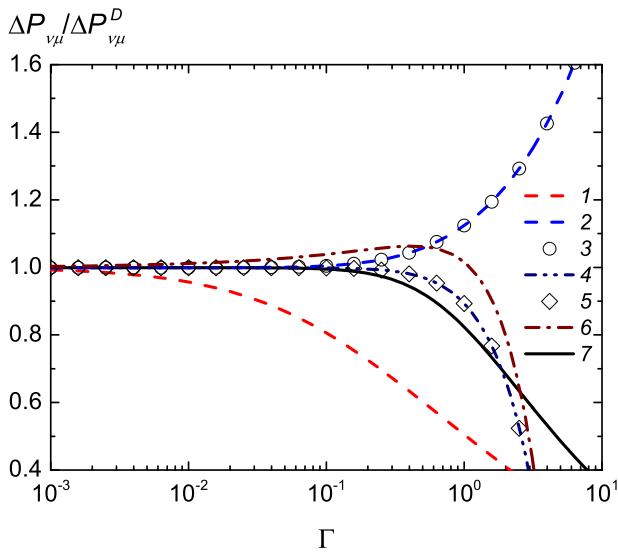
FIG. 10. The partial (curves 1–6, reduced to the partial Debye pressure correction, see Fig. 9) and the full pressure correction (curve 7) vs the coupling parameter for $n_0 = 10^5$ cm^{-3}, $n_2 = 10^8$ cm^{-3}, $\overline{T} = 300$ K, and $z_0 < 0$.

The contribution due to the interaction of dust particles with each other is the first to deviate from the Debye approximation. Moreover, the full correction coincides well with the Debye correction up to $\Gamma \sim 0.1$, and then the deviations grow quickly.

The data presented in Figs. 9 and 10 imply that the full correction and the correction ΔP_{00} turn out to be negative, as in the Debye approximation, in the entire studied range of the coupling parameter. In Refs. 25 and 26, the positive pressure corrections were obtained while considering a system of dust particles interacting with a Debye potential. The opposite sign of the corrections is due to the fact that in these papers, the pressure was calculated with the Debye potential, and in the present work, it is estimated with the Coulomb potential. As it is shown above, the introduction of the Debye potential (with a screening constant taking into account the contribution of electrons and ions only) is a convenient mathematical method for calculating the pair correlation function of dust particles h_{00} in the case when the interactions of dust particles with electrons and ions, electrons between themselves and ions, the ions between them are ideal. In this case, the real interaction potential of charged particles remains the Coulomb one.

VIII. THERMODYNAMIC STABILITY OF DUSTY PLASMAS

It was noted above that the appearance of negative SDF values is associated with the instability of the system and the possibility of a transition to a new phase state. Therefore, the thermodynamic stability (TDS) of a dusty plasma is to be studied. Consider the system as a solution: dust particles are particles of a substance dissolved in an electron–ion plasma, while electrons and ions are particles of a solvent. In this case, the following conditions must be satisfied for the TDS of a dusty plasma:[47,61]

$$C_V = \left(\frac{\partial U}{\partial T}\right)_{V, N_0, N_1, N_2} > 0, \tag{51}$$

$$K_T = -\frac{1}{V}\left[\left(\frac{dP}{dV}\right)_{T, N_0, N_1, N_2}\right]^{-1} > 0, \tag{52}$$

$$\mu_{00} > 0, \quad \mu_{11} > 0, \quad \mu_{00}\mu_{11} - \mu_{01}\mu_{10} > 0. \tag{53}$$

Here, C_V and K_T are the isochoric heat capacity and the isothermal compressibility of the plasma, respectively, and $\mu_{\nu\lambda}$ are the derivatives of the ν-species chemical potential with respect to the number of λ-species particles,

$$\mu_{\nu\lambda} = \mu_{\lambda\nu} = \left(\frac{\partial \mu_\nu}{\partial N_\lambda}\right)_{P, T, N_\tau, \tau \neq \lambda}.$$

The interaction corrections to the isochoric heat capacity, $\Delta C_V = C_V - C_{V,id}$, $C_{V,id} = \frac{3}{2}nk_B$, divided by ΔC_V^D [see Eq. (54)] are shown in Fig. 11. In the Debye approximation, the heat capacity at a constant volume is determined by the following expression:

$$C_V^D = C_{V,id} + \Delta C_V^D = nk_B\left(\frac{3}{2} + \frac{\beta e^2 k_D}{4n}\sum_\nu n_\nu z_\nu^2\right). \tag{54}$$

One can see from Eq. (54) that in the Debye approximation, ΔC_V^D is positive and monotonically increases with growing Γ and z_0, reaching the value of $2.72 nk_B$ at $\Gamma = 221.3$ in the dusty plasma with $z_0 < 0$ and $1.27 nk_B$ for $\Gamma = 278.6$ in the dusty plasma with $z_0 > 0$; $\Gamma = 221.3$ and $\Gamma = 278.6$ are the maximum values of the coupling parameter, above which the iterations of the OZ equation did not converge after 2000 iterations.
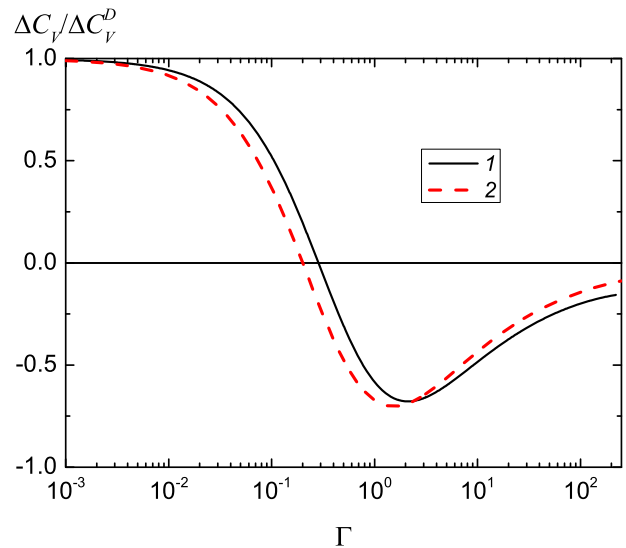
FIG. 11. The interaction correction to the ideal isochoric heat capacity reduced to the Debye one (54) for a multicomponent dusty plasma vs the coupling parameter. Curve 1 corresponds to $n_0 = 10^5$ cm^{-3}, $n_2 = 10^8$ cm^{-3}, $\overline{T} = 300$ K, and $z_0 < 0$; curve 2 is for $n_0 = 10^7$ cm^{-3}, $n_2 = 10^{10}$ cm^{-3}, $\overline{T} = 2000$ K, and $z_0 > 0$.

From Fig. 11, it can be seen that for small Γ, ΔC_V and ΔC_V^D are close to each other, with increasing Γ, they begin to differ more and more, and for $\Gamma \approx 0.82$ in the dusty plasma with $z_0 < 0$ and for $\Gamma \approx 0.20$ in the dusty plasma with $z_0 > 0$, the correction due to the interaction, ΔC_V, becomes negative. Furthermore, ΔC_V monotonically increases in absolute value, reaching the values of $\Delta C_V = -0.426 n k_B$ at $\Gamma = 221.3$ in the dusty plasma with $z_0 < 0$ and $\Delta C_V = -0.105 n k_B$ at $\Gamma = 278.6$ in the dusty plasma with $z_0 > 0$. It can be concluded that, taking into account the ideal component [see Eq. (54)], the isochoric specific heat of dusty plasma is positive in the entire investigated range of the coupling parameter values and that the first TDS condition (51) is fulfilled.

Figure 12 shows the values of the isothermal compressibility of a dusty plasma,

$$K_T = -\frac{1}{V}\left[\left(\frac{dP}{dV}\right)_T\right]^{-1} = \left[n\left(\frac{\partial P}{\partial n}\right)_T\right]^{-1}, \tag{55}$$

obtained by the numerical solution of the OZ equation in the HNC approximation and in the Debye approximation. From Eq. (45), for the isothermal compressibility in the Debye approximation, one finds

$$K_T^D = \left(1 - \frac{k_D^3}{16\pi n}\right)^{-1}. \tag{56}$$

It can be deduced from Fig. 12 that for small values of the coupling parameter, the values of K_T calculated on the basis of the solution of the OZ equation in the HNC approximation and in the Debye approximation practically coincide, but at $\Gamma > 0.01$, the curves begin to diverge. The isothermal compressibility values

$$\eta = K_T n T - 1$$
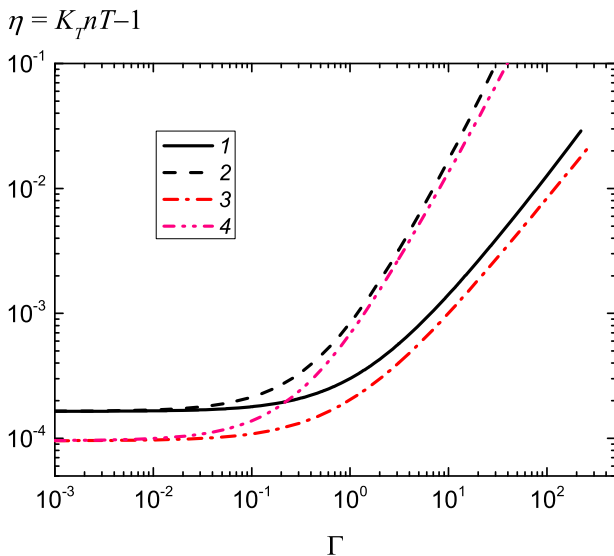
FIG. 12. Isothermal compressibility of a multicomponent dusty plasma as a function of coupling parameter. Curves 1 and 2 are for $n_0 = 10^5$ cm^{-3}, $n_2 = 10^8$ cm^{-3}, $\overline{T} = 300$ K, and $z_0 < 0$; curves 3 and 4 are for $n_0 = 10^7$ cm^{-3}, $n_2 = 10^{10}$ cm^{-3}, $\overline{T} = 2000$ K, and $z_0 > 0$. Curves 1 and 3 were calculated from the solution of the OZ equation in the HNC approximation, and curves 2 and 4 were calculated in the Debye approximation from Eq. (48).

calculated from the OZ equation in the HNC approximation are higher than unity and remain finite in the entire studied range of Γ. In the Debye approximation, K_T for the plasma parameters considered here passes (through infinity) to the region of negative values for $\Gamma \approx 128$ for the dusty plasma with $z_0 < 0$ and for $\Gamma \approx 229$ for the dusty plasma with $z_0 > 0$. Therefore, we can conclude that the isothermal compressibility of dusty plasma is positive in the entire studied range of the coupling parameter, and the second TDS condition (52) is also satisfied.

Consider now TDS conditions (53) with respect to the species chemical potentials. Since the determination of the chemical potential in numerical calculations encounters certain difficulties, define it first in the Debye approximation based on the free energy, which, in the Debye approximation, is determined by the following expression:[47]

$$F = -\sum_\nu N_\nu T \ln\left[g_\nu \frac{eV}{N_\nu}\left(\frac{m_\nu T}{2\pi\hbar^2}\right)^{3/2}\right] - \frac{2e^3}{3}\sqrt{\frac{\pi}{TV}}\left(\sum_\nu N_\nu z_\nu^2\right)^{3/2}, \tag{57}$$

where g_ν is the degeneracy multiplicity of particles of the component ν and e under the logarithm is the base of the natural logarithm. For the chemical potential of the component ν from Eq. (57), one has

$$\mu_\nu = \left(\frac{\partial F}{\partial N_\nu}\right)_{T,V,N_{\tau,\tau\neq\nu}}$$

$$= -T\ln\left[g_\nu \frac{V}{N_\nu}\left(\frac{m_\nu T}{2\pi\hbar^2}\right)^{3/2}\right] - e^3\sqrt{\frac{\pi}{TV}}z_\nu^2\left(\sum_\nu N_\nu z_\nu^2\right)^{1/2}. \tag{58}$$

Using Eq. (45) to determine $\partial V/\partial N_\nu$, from (58), it can be found that

$$\left(\frac{\partial\mu_\lambda}{\partial N_\nu}\right)_{P,T,N_{\tau,\tau\neq\nu}} = \frac{T}{N_\nu}\left(\delta_{\nu\lambda} - \frac{e^2 z_\lambda^2 k_\nu^2}{4k_D T}\right)$$
$$- \frac{1}{V}\frac{\left(T - \frac{1}{4}e^2 z_\nu^2 k_D\right)\left(T - \frac{1}{4}e^2 z_\lambda^2 k_D\right)}{\frac{3}{2}P - \frac{1}{2}nT}. \tag{59}$$

Therefore, the thermodynamic stability of the dusty plasma is determined by the sign of the dimensionless parameters ζ_ν, $\nu = 0, 1$, defined as

$$\zeta_\nu = \frac{N_\nu}{T}\mu_{\nu\nu} = \left(1 - \frac{\beta e^2 z_\nu^2 k_\nu^2}{4k_D}\right) - \frac{n_\nu}{8n}\frac{\left(4 - \beta z_\nu^2 k_D e^2\right)^2}{(3P\beta/n - 1)}, \tag{60}$$

and by the sign of the dimensionless parameter ζ_{01} defined as

$$\zeta_{01} = \frac{2N_0 N_1}{T^2}\left(\mu_{00}\mu_{11} - \mu_{01}\mu_{10}\right)$$

$$= \frac{2n_2}{n}\left(1 - \frac{k_D^3}{16\pi n}\right)^{-1}\left(1 - \frac{e^2 k_D}{4T}\frac{\sum_\nu n_\nu z_\nu^4}{\sum_\nu n_\nu z_\nu^2}\right). \tag{61}$$

Note that the second term on the right-hand side of Eq. (60) for $\nu = 0$ is determined by the ratio n_0/n, and therefore, in the sign change region and in the calculations performed in this paper, this contribution is three orders of magnitude smaller than unity and can be omitted in the analysis of ζ_0.

Norman and Starostin observed in Ref. 59 that the third condition (53) can be reduced to the requirement of stability of a nonideal subsystem without taking into account the ideal subsystems,

for which the isothermal compressibility must be positive,

$$K_{T,00} = -\frac{1}{V}\left[\left(\frac{\partial P_{00}}{\partial V}\right)_T\right]^{-1}. \tag{62}$$

Here, as the pressure of the dust subsystem, the component P_{00} is used, as it is commonly done in the one-component approximation.

In the Debye approximation, the isothermal compressibility of the dust subsystem is defined as

$$K_{T,00}^D = \frac{\beta}{n_0}\left(1 - \frac{\beta e^2 z_0^2 k_0^2}{4k_D}\right)^{-1}. \tag{63}$$

It is the positivity condition of $K_{T,00}$ that is employed to determine the thermodynamic stability in the one-component approximation.

A comparison of ζ_0, ζ_{01}, and $\chi_{00}^D = 1/\left(K_{T,00}^D n_0 T\right)$ in the Debye approximation is performed in Fig. 13. It should be noted that ζ_0 and ζ_{01} practically coincide. A very good correlation is observed in the behavior of these quantities as functions of Γ, and the points of change of their sign are close to each other. The reason for this is that the expression in the parentheses in (63) coincides with the first term in Eq. (60) for $v = 0$, which, as we noted above, is the dominant term. Figure 13 also shows the dependence of the isothermal compressibility of the dust subsystem, obtained from the following expression for pressure [the term with $v = 0$ in Eq. (45)],

$$P_0 = n_0 T - \frac{1}{6}e^2 k_D n_0 z_0^2, $$

while the isothermal compressibility is determined as

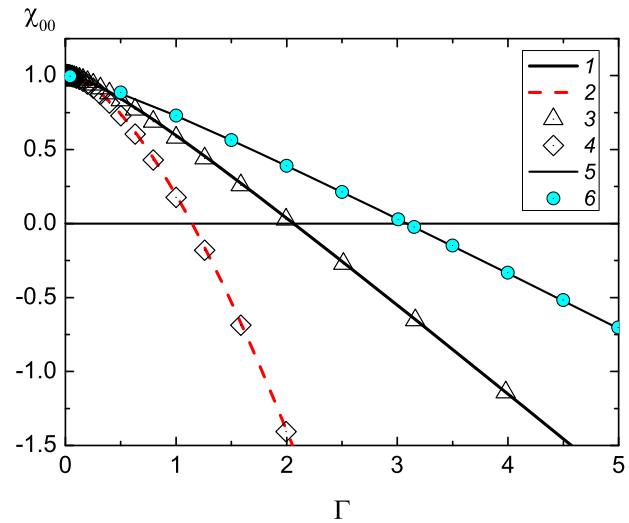$$K_{T,0}^D = \frac{1}{n_0 T}\left(1 - \frac{e^2 z_0^2 k_D}{4T}\right)^{-1}. \tag{64}$$
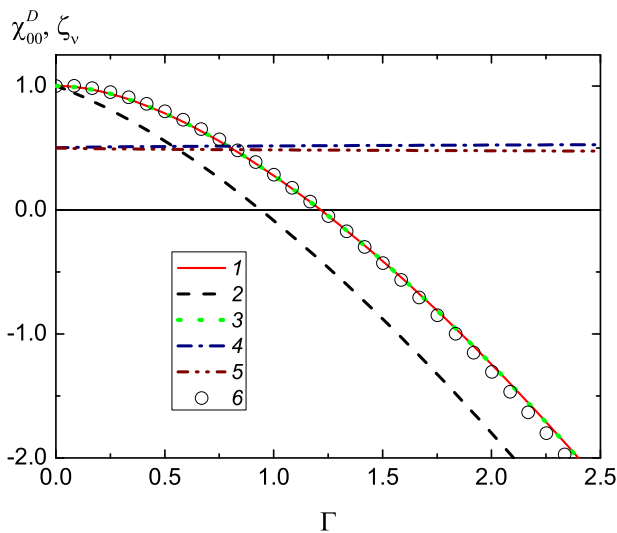
As it follows from Fig. 13, the behavior of the latter quantity correlates somewhat worse with that of ζ. Therefore, below, as the third condition of the TDS of the dusty plasma, the positivity of $K_{T,00}$ is used.

The isothermal compressibility of the plasma dust subsystem found on the basis of the numerical solution of the OZ equation in the HNC approximation is shown in Fig. 14 as a function of the coupling parameter. It can be seen that the values of $K_{T,00}$ become negative both in the calculation based on the solution of the OZ equation in the HNC approximation (at $\Gamma \approx 2$) and in the Debye approximation (at $\Gamma \approx 1$). The values of $K_{T,00}$ for both sets of plasma parameters with negative and positive charges of dust particles considered here are accidental close to each other. Indeed, it can be seen from Eq. (63) that the critical value of the non-ideality parameter, at which the isothermal compressibility of the dust subsystem becomes negative, is determined in the Debye approximation by the expression

$$\Gamma_{D,cr} = \sqrt{k_{D^a}/\pi}. \tag{65}$$

The dependence of this critical value on the plasma parameters was confirmed by the numerical solutions of the OZ equation in the HNC approximation. A detailed study of this issue will be carried out in a separate work.

It was shown in Ref. 55 that in the one-component approximation, the isothermal compressibility of dusty plasmas becomes negative at $\Gamma \approx 3$ (see Fig. 14 and Ref. 18), which is close enough to the data obtained in the present work. Filippov *et al.*[55] calculated the isothermal compressibility using the equation of state of

FIG. 13. Inverse isothermal compressibility $\chi_{00}^D = \left(K_{T,00}^D n_0 T\right)^{-1}$, the derivatives of the chemical potential ζ_v (60) and ζ_{01} (61) in the Debye approximation vs the coupling parameter for $n_0 = 10^5$ cm^{-3}, $n_2 = 10^8$ cm^{-3}, $\overline{T} = 300$ K, and $z_0 < 0$ with curves 1, 2, 3, 4, 5, and 6 standing for $\eta = K_{T,00}n_0T$, $\eta = K_{T,0}n_0T$, ζ_0, ζ_1, ζ_2, and ζ_{01}, respectively.

FIG. 14. Inverse isothermal compressibility of the plasma dust component $\chi_{00} = \left(K_{T,00}n_0T\right)^{-1}$ as a function of the coupling parameter: curves 1 and 2 are for $n_0 = 10^5$ cm^{-3}, $n_2 = 10^8$ cm^{-3}, $\overline{T} = 300$ K, and $z_0 < 0$; curves 3 and 4 are for $n_0 = 10^7$ cm^{-3}, $n_2 = 10^{10}$ cm^{-3}, $\overline{T} = 2000$ K, and $z_0 > 0$; curves 1 and 3 are from the solution of the OZ equation in the HNC approximation, curves 2 and 4 are in the Debye approximation Eq. (63), curve 5 is calculated from Eq. (66), and curve 6 is calculated using the OCP equation of state obtained by numerical simulation of the OZ equation in the HNC approximation.[55]

a one-component plasma (OCP). It was done by numerical simulation of the OZ equation in the HNC approximation and with the Coulomb potential used as the interaction potential between dust particles. For this reason, the results of Ref. 55 differ from the data obtained in the present paper. It can be seen in Fig. 14 that the results of that paper are closely described by the Baus and Hansen formula[62]

$$\chi_{00} = 1 + \frac{4}{9}a\Gamma + \frac{13}{36}b\Gamma^{1/4} + \frac{1}{3}c,$$

$$a = -0.896\,43, \ b = 0.861\,85, \ c = -0.5551,$$

(66)

obtained by the least-square fit to the MD data over the entire fluid range $1 \leq \Gamma \leq 160$.

Negative values of $K_{T,00}$ indicate that the third TDS condition (53) in dusty plasmas is violated and that they are thermodynamically unstable at high values of the coupling parameter $\Gamma \gtrsim 2$. We note that the stabilization of the dust subsystem can be achieved, for example, upon taking into account the finite size of dust particles. The thermodynamical instability of the dust component can lead to its stratification with the formation of two regions with different densities, in one of which the dust particles would form a close-packed lattice. This is similar to the phase separation of sodium-ammonia solutions with increasing solution concentration that results in a very abrupt reduction of the value of the dielectric constant real part to large (by its module) and negative values.[63] This decrease can be interpreted as a metal-to-nonmetal transition associated with a very rapid decrease in the mass of negatively charged carriers as the concentration increases.

As it can be seen from Fig. 15, the pressure of the dust subsystem as a function of the number density of dust particles passes through a maximum for all charges considered in this figure: at $n_0 = 7.24 \times 10^5 \ cm^{-3}$ and $\Gamma = 1.93$ for curve 1, at $n_0 = 1.07 \times 10^5 \ cm^{-3}$
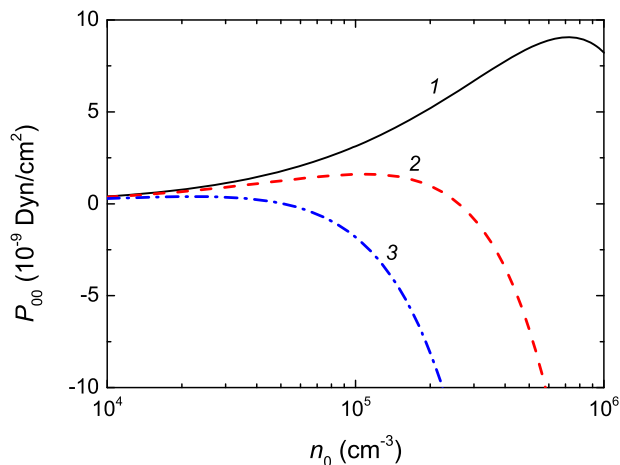
and $\Gamma = 2.05$ for curve 2, and at $n_0 = 2.24 \times 10^4 \ cm^{-3}$ and $\Gamma = 2.43$ for curve 3. It is at these points that the isothermal compressibility becomes infinite and changes sign.

IX. CONCLUSIONS

In the present work, on the basis of the Ornstein–Zernike equation for a multicomponent plasma, a transition is described to a one-component plasma approximation with an effective pseudopotential and in order to calculate the dust–dust pair correlation function. It was established that in the case when all subsystems except the dust one are ideal, the effective pseudopotential becomes the Debye potential with the screening constant, which should be determined without the contribution of the dust subsystem but taking into account the condition of the total plasma quasineutrality. If the non-dust components are not ideal, the above effective potential might deviate from the Debye form. In other words, we do not initially model the dusty plasma as a Yukawa one-component system applicable only when all components are weakly coupled. This conclusion is also important for the problem of determining the Coulomb logarithm in dense plasmas, where there is a problem of choosing the screening constant while calculating the ion correlations (see Ref. 64 and references therein). In light of the present work, it is concluded that while considering the inter-ion correlations, only the screening by the electrons should be taken into account.

It is also shown that for $\Gamma > 1$, the static dielectric function of the plasma becomes negative for small values of the wavenumber k, and as Γ grows, this negativity region expands noticeably. Therefore, screening in non-ideal plasmas is not described by the Debye theory. The negativity of the SDF leads to the appearance of a range of distances, where the attraction of particles with charges of the same sign and the repulsion of particles with charges of the opposite sign are observed. In this case, the depth of the well in the interaction potential increases with the growing coupling parameter, and the barrier height also grows from the side of large distances.

The separation of the effective dusty subsystem has permitted us to carry out a detailed study of its thermodynamic properties, and it has been found that the contribution to pressure due to interactions in the entire investigated range of the coupling parameter $\Gamma < 300$ has a negative sign, but both the total pressure and the isothermal compressibility remain positive.

It has also been shown that the isothermal compressibility of the dusty non-ideal subsystem becomes negative at $\Gamma \approx 2$ in the realm of variation of the plasma parameters considered here both in dusty plasmas (in thermal equilibrium) with negative and positive charges. Within the *ab initio* Coulomb model of the system containing the dust particles, this instability is presumably related to the appearance of the attractive part of the effective interaction potential. Certainly, the question of the thermodynamic stability of dusty plasmas requires further study, taking into account its openness and nonequilibrium nature. Such a study, as well as a detailed analysis of alternative results on the thermodynamic properties of dusty plasmas, for example, based on the Debye–Hückel plus hole (DHH) approximation,[20] will be carried out elsewhere. Note, finally, that the results obtained in this paper are also applicable in the theory of electrolytes.

FIG. 15. Equation of state of the dusty component for $n_2 = 10^8 \ cm^{-3}$, $T = 300$ K, and $z_0 < 0$: curve 1 is calculated with $z_0 = -62.192$, 2 with $z_0 = -87.953$, and 3 with $z_0 = -124.38$. These charges at $n_0 = 10^5 \ cm^{-3}$ correspond to the values of the coupling parameter $\Gamma = 1$, 2, and 4, respectively.

REFERENCES

[1] V. N. Tsytovich, Phys.-Usp. **40**, 53 (1997).

[2] V. E. Fortov, A. G. Khrapak, S. A. Khrapak, V. I. Molotkov, and O. F. Petrov, Phys.-Usp. **47**, 447 (2004).

[3] V. Fortov, A. Ivlev, S. Khrapak, A. Khrapak, and G. Morfill, Phys. Rep. **421**, 1 (2005).

[4] I. Mann, N. Meyer-Vernet, and A. Czechowski, Phys. Rep. **536**, 1 (2014).

[5] P. K. Shukla and A. A. Mamun, *Introduction to Dusty Plasma Physics* (CRC Press, 2015).

[6] F. Greiner, A. Melzer, B. Tadsen, S. Groth, C. Killer, F. Kirchschlager, F. Wieben, I. Pilch, H. Krüger, D. Block, A. Piel, and S. Wolf, Eur. Phys. J. D **72**, 81 (2018).

[7] A. Ivlev, H. Löwen, G. Morfill, and C. P. Royall, in *Series in Soft Condensed Matter*, Complex Plasmas and Colloidal Dispersions: Particle-Resolved Studies of Classical Liquids and Solids Vol. 5 (World Scientific, Singapore, 2012).

[8] A. V. Filippov, A. F. Pal', and A. N. Starostin, J. Exp. Theor. Phys. **121**, 909 (2015).

[9] F. Babick, "Fundamentals in colloid science," in *Suspensions of Colloidal Particles and Aggregates*, Particle Technology Series Vol. 20 (Springer International Publishing, Cham, 2016), pp. 75–118.

[10] H. Ohshima, "Electrostatic interaction between colloidal particles," in *Encyclopedia of Biocolloid and Biointerface Science 2V Set* (John Wiley & Sons, Inc., Hoboken, NJ, USA, 2016).

[11] A. V. Filippov and I. N. Derbenev, J. Exp. Theor. Phys. **123**, 1099 (2016).

[12] I. N. Derbenev, A. V. Filippov, A. J. Stace, and E. Besley, J. Chem. Phys. **145**, 084103 (2016).

[13] C. Chen and W. Huang, Environ. Sci. Technol. **51**(4), 2077 (2017).

[14] V. E. Fortov and G. E. Morfill, *Complex and Dusty Plasmas* (Taylor & Francis, London, 2009).

[15] S. Hamaguchi and R. T. Farouki, J. Chem. Phys. **101**, 9876 (1994).

[16] R. T. Farouki and S. Hamaguchi, J. Chem. Phys. **101**, 9885 (1994).

[17] S. Hamaguchi, R. T. Farouki, and D. H. E. Dubin, Phys. Rev. E **56**, 4671 (1997).

[18] H. Totsuji, Phys. Plasmas **15**, 072111 (2008).

[19] H. Totsuji, Microgravity Sci. Technol. **23**, 159 (2011).

[20] S. A. Khrapak, A. G. Khrapak, A. V. Ivlev, and G. E. Morfill, Phys. Rev. E **89**, 023102 (2014).

[21] S. A. Khrapak, G. E. Morfill, A. V. Ivlev, H. M. Thomas, D. A. Beysens, B. Zappoli, V. E. Fortov, A. M. Lipaev, and V. I. Molotkov, Phys. Rev. Lett. **96**, 015001 (2006).

[22] P. Debye and E. Hückel, Phys. Z. **24**, 185 (1923).

[23] J.-P. Hansen and I. R. McDonald, *Theory of Simple Liquids* (Elsevier, London, 2006).

[24] G. N. Sarkisov, Phys.-Usp. **42**, 545 (1999).

[25] V. V. Reshetniak, A. N. Starostin, and A. V. Filippov, J. Exp. Theor. Phys. **127**, 1153 (2018).

[26] V. V. Reshetniak and A. V. Filippov, J. Exp. Theor. Phys. **129**, 459 (2019).

[27] J. P. Hansen, G. M. Torrie, and P. Vieillefosse, Phys. Rev. A **16**, 2153 (1977).

[28] S. Ichimaru, Rev. Mod. Phys. **54**, 1017 (1982).

[29] B. Beresford-Smith, D. Y. Chan, and D. J. Mitchell, J. Colloid Interface Sci. **105**(1), 216 (1985).

[30] S. Ichimaru, H. Iyetomi, and S. Tanaka, Phys. Rep. **149**, 91 (1987).

[31] M. Fushiki, J. Chem. Phys. **89**, 7445 (1988).

[32] V. Schwarz, T. Bornath, W.-D. Kraeft, S. H. Glenzer, A. Höll, and R. Redmer, Contrib. Plasma Phys. **47**(4–5), 324 (2007).

[33] K. Wünsch, P. Hilse, M. Schlanges, and D. O. Gericke, Phys. Rev. E **77**(5), 056404 (2008).

[34] R. Bredow, T. Bornath, W.-D. Kraeft, and R. Redmer, Contrib. Plasma Phys. **53**, 276 (2013).

[35] M. W. C. Dharma-wardana, Phys. Rev. B **100**, 155143 (2019).

[36] A. V. Filippov, V. V. Reshetnyak, A. N. Starostin, I. M. Tkachenko, and V. E. Fortov, JETP Lett. **110**, 659 (2019).

[37] B. V. Zelener, G. E. Norman, and V. S. Filinov, High Temp. **13**, 650 (1975).

[38] G. Kelbg, Ann. Phys. **467**, 219 (1964).

[39] G. Kelbg, Ann. Phys. **467**, 354 (1964).

[40] Yu. L. Klimontovich and W.-D. Kraeft, High Temp. Sci. **12**, 212 (1974).

[41] C. Deutsch, Phys. Lett. **60**, 317 (1977).

[42] C. Deutsh, M. M. Gombert, and H. Minoo, Phys. Lett. A **66**, 381 (1978); **72**, 481 (1979).

[43] A. E. Davletov, L. T. Yerimbetova, Yu.V. Arkhipov, Ye. S. Mukhametkarimov, A. Kissan, and I. M. Tkachenko, J. Plasma Phys. **84**, 905840410 (2018).

[44] L. T. Yerimbetova, A. E. Davletov, Y. V. Arkhipov, and I. M. Tkachenko, Contrib. Plasma Phys. **59**, e201800160 (2019).

[45] N. R. Shaffer, S. K. Tiwari, and S. D. Baalrud, Phys. Plasmas **24**, 092703 (2017).

[46] S. Ichimaru, in *Statistical Plasma Physics*, Basic Principles Vol. I (Addison Wesley Publishing Company, Redwood, California, USA, 1992).

[47] L. D. Landau and E. M. Lifshitz, in *Course of Theoretical Physics*, Statistical Physics: Part 1 Vol. 5 (Pergamon, Oxford, 1980).

[48] D. Pines and P. Nozières, *Theory of Quantum Liquids* (W.A. Benjamin, Inc., New York, Amsderdam, 1966), Sec. 2.1.

[49] E. G. Maksimov and O. V. Dolgov, Phys.-Usp. **50**, 933 (2007).

[50] O. V. Dolgov, D. A. Kirzhnits, and E. G. Maksimov, Rev. Mod. Phys. **53**, 81 (1981).

[51] A. F. Alexandrov, L. S. Bogdankevich, and A. A. Rukhadze, in *Principles of Plasma Electrodynamics*, Springer Series Electrophys. Vol. 9 (Springer, Berlin, 1984).

[52] *High-temperature Superconductivity*, edited by V. L. Ginzburg and D. A. Kirzhnits (Consultants Bureau, New York and London, 1982).

[53] K. C. Ng, J. Chem. Phys. **61**, 2680 (1974).

[54] A. V. Filippov, A. N. Starostin, I. M. Tkachenko, and V. E. Fortov, Phys. Lett. A **376**, 31 (2011).

[55] A. V. Filippov, A. N. Starostin, I. M. Tkachenko, and V. E. Fortov, Contrib. Plasma Phys. **53**(4-5), 442 (2013).

[56] V. E. Fortov, A. P. Nefedov, O. F. Petrov, A. A. Samarian, A. V. Chernyschev, and A. M. Lipaev, JETP Lett. **63**, 187 (1996).

[57] V. E. Fortov, A. P. Nefedov, O. F. Petrov, A. A. Samarian, and A. V. Chernyschev, Phys. Rev. E **54**, R2236 (1996).

[58] V. E. Fortov, V. S. Filinov, A. P. Nefedov, O. F. Petrov, A. A. Samaryan, and A. M. Lipaev, J. Exp. Theor. Phys. **84**, 489 (1997).

[59] G. E. Norman and A. N. Starostin, High Temp. **6**, 394 (1968).

[60] G. E. Norman and A. N. Starostin, High Temp. **8**, 381 (1970).

[61] I. Prigogine and R. Defay, *Chemical Thermodynamics* (Longmans Green & Co., London, NY, Toronto, 1954).

[62] M. Baus and J.-P. Hansen, Phys. Rep. **59**, 1 (1980).

[63] D. W. Mahaffey and D. A. Jerde, Rev. Mod. Phys. **40**(4), 710 (1968).

[64] A. V. Filippov, A. N. Starostin, and V. K. Gryaznov, J. Exp. Theor. Phys. **126**, 430 (2018).